Non-Arrhenius relaxation in micromagnetic models of systems with many degrees of freedom

J. M. González, R. Ramírez, and R. Smirnov-Rueda
Institito de Ciencia de Materiales de Madrid del Consejo Superior de Investigaciones Científicas, Serrano 144, 28006 Madrid, Spain

J. González
Departamento de Física de Materiales, Facultad de Ciencias Químicas, Universidad del País Vasco, 20009 San Sebastián, Spain
(Received 6 July 1995)

We present results corresponding to the simulation of the relaxation of simple magnetic systems consisting of isolated and coupled grains. Those results, obtained in the framework of the micromagnetic approximation, evidence remarkable differences with the classical two-level system predictions in which the experimental treatment of the magnetic viscosity phenomenology is based. In particular, we show the existence of a "waiting time" required to nucleate the well-defined magnetic moment structures which are responsible for the change of the global state of the system. In addition to this, we observe the occurrence of nonequivalent relaxation trajectories.

I. INTRODUCTION

As is well known[1] the phenomenology of magnetic hysteresis is based on the occurrence of what is commonly called "a distribution of energy barriers" which protects the remanent-type magnetization configurations from decaying towards the reversed states (those corresponding to a global magnetization pointing essentially along the sense of the demagnetizing field). It is also known that the particular characteristics of that "distribution of energy barriers" depend on the field value as well as on intrinsic (i.e., anisotropy, saturation magnetization, etc.) and extrinsic properties (linked, as a general feature, to defects).[2] At finite temperatures and constant applied demagnetizing fields, thermal fluctuations can induce an irreversible change of the magnetization direction by making the system overcome the barriers.[3] This phenomenology has been experimentally observed and discussed in a wide variety of materials.[4–10] In principle, and assuming that the basic magnetization reversal mechanism is known, the analysis of the experimental data corresponding to the time evolution of the magnetization could yield information about some of the characteristics of the distribution of energy barriers.[3]

Nevertheless, and even in the case of samples having well-controlled crystallochemical and microstructural properties, the correlation of the experimental information on magnetization relaxation (magnetic viscosity) with the particular structured and morphological characteristics is far from being clear.[11] In the present work, trying to get a deeper insight into this correlation, we have modeled, in terms of the micromagnetic approximation, the evolution from the metastable to the minimum-energy states of very simple magnetic systems.

To end this Introduction we should point out that, unlike previous simulations,[12,13] our approach allows the validity of Arrhenius kinetics[14] for the elemental processes involved in the time evolution of the magnetization (i.e., those corresponding to the overcoming of a local energy barrier) to be examined. That kinetics is the key assumption for most of the phenomenological treatments of the magnetization viscosity[15,16] and it is linked to the possibility of describing the relaxing system in terms of a reduced number of degrees of freedom. Since, with just a few exceptions, the hysteretic behavior of real materials shows large departures from the predictions of the Stoner-Wohlfarth demagnetization mechanism,[17] which is only compatible with that reduced number of degrees of freedom, we will emphasize the consequences of considering a larger number of them.

II. DESCRIPTION OF THE MODEL AND RESULTS

Our model of a relaxing magnetic system consists of a long chain of parallel infinite planes, each one representing an atomic plane in a real material. The concrete number of planes is, in every case, the minimum required to get, to a sufficient approximation, weakly size-dependent results for the system under consideration. As a general feature the total size of the system is one order of magnitude larger than the correlation length relevant for the particular problem. For the sake of simplicity, intraplane and interplane exchange constants are considered infinite and finite, respectively [which renders our model one dimensional (1D), although the magnetic moments associated with each plane are allowed to orient in 3D]. Local magnetic properties are defined by (1) the exchange-to-anisotropy ratio, $a = Ad^{-2}/K$ (where A, d, and K are the exchange constant, the interplanar distance, and the anisotropy constant, respectively); (2) the square of the magnetization-to-anisotropy ratio, $m = \mu_0 M_S^2/2K$ (where M_S is the saturation magnetization); and (3) the local easy-axis orientation. Grain boundaries are defined by discontinuities in the local easy-axis orientation. A coefficient g, representing the grain boundary structure, is used as intergrain exchange coupling coefficient. In all cases we consider values of the above parameters which correspond to highly anisotropic materials. The internal energy of the system includes the anisotropy energy (local, uniaxial), the Zeeman energy (local, unidirectional), and the exchange energy (first neighbors), as well as the magnetostatic energy (many-body interaction although in 1D it can be reduced to a local form). Explicitly, the total internal energy E_T is written as[18]

$$E_T \propto \frac{1}{2}\sum_{i=1}^{N} \sin^2[\arccos(\mathbf{u}_{mi}\cdot\mathbf{u}_{ki})] - H_{\mathrm{app}}\sum_{i=1}^{N} \mathbf{u}_{mi}\cdot\mathbf{u}_H - a\sum_{i=1}^{N-1} \mathbf{u}_{mi}\cdot\mathbf{u}_{m(i+1)} + m\sum_{i=1}^{N} (\mathbf{u}_{mi}\cdot\mathbf{u}_y)^2.$$

Here $\mathbf{u}_{mi}$, $\mathbf{u}_{ki}$, $\mathbf{u}_H$, and $\mathbf{u}_y$ are unit vectors along the directions of the moment at the ith position in the chain representing the system, the easy axis corresponding to that position, the applied field, and the OZ axis of the considered reference system, respectively. The applied field H is expressed as $H_{\mathrm{app}}=\mu_0 M_S H/2K$.

The evolution of the total internal energy is followed by a Monte Carlo algorithm with Metropolis dynamics in a canonical ensemble (at a temperature corresponding to 2×10^{-4} of the maximum anisotropy energy attainable by the system). We define a Monte Carlo step (MCS) as the process corresponding to the consecutive introduction of random modifications (moves) in all the degrees of freedom of the system. If the attempt frequency (that is, the time rate at which a real system can modify its degrees of freedom) is known (through independent physical arguments) the number of Monte Carlo steps can be converted into time units. The bounds for the modification of the degrees of freedom of the system (two angles for the magnetic moment representing each plane) are arbitrarily chosen so as to result in a percentage of accepted moves of the order of 50%. Finally, as we are studying transitions from a well-defined initial state (saturation) to a well-defined final state (globally reversed magnetization state) neither initial configuration averages nor termination criteria are required.

A. Relaxation of an isolated grain

In the following we discuss the relaxation of three different simple systems: an isolated grain, a system with short-range coupling, and, finally, a system with many-body interactions. Consider a single-grain system (A), in which the easy-axis direction and the magnitude of all the other local magnetic properties are independent of the position. After initial saturation along the positive OZ axis (that of the easy direction, see Fig. 1), a demagnetizing field H_{app} pointing along the negative OZ axis is applied and the system is allowed to relax.

The evolution of the reduced magnetization of the system with the number of MCS's is shown in Fig. 1 for $a=5$, $m=0.15$, $d=2.5\times10^{-10}$ m, and $H_{\mathrm{app}}=1.1$. A range of MCS's exists in which the fluctuations in the orientation of the magnetic moments representing each plane (simulated by means of the Monte Carlo algorithm) do not lead to any macroscopic change in the state of the system. After this, a region of reversed magnetization is nucleated and magnetization reversal proceeds through displacement of 180° domain-wall-like structures which sweep through the system. A relevant consequence of this is the fact that dissipation should occur during the propagation of these structures, which will lead to the occurrence of different proportionality constants between real time and the number of MCS's for the different relaxation stages in Fig. 1.

These nucleation and propagation processes are illustrated in Fig. 2 where the components along the field direction of

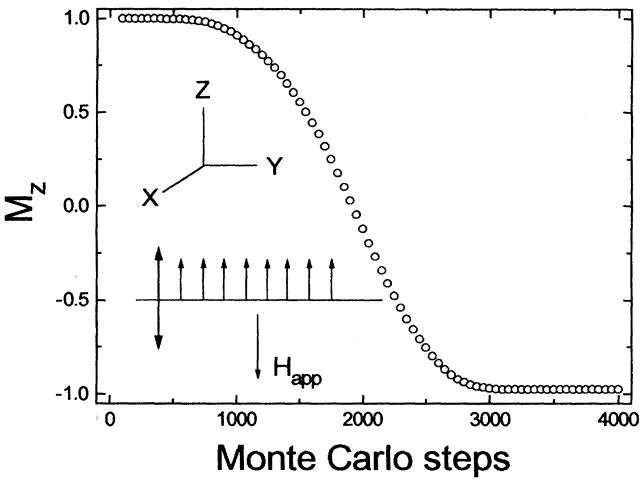

FIG. 1. System A. Typical example of the evolution of the reduced magnetization with the number of MCS's. Magnetization is measured along the OZ direction and it is considered positive when it points antiparallel to the applied magnetic field.

the magnetic moments representing the different planes in the system are plotted for different relaxation stages. It is important to note that nucleation occurs preferentially at the edges of the system, although this fact is influenced by the considered value of the bound used for the random modification of the local moment orientation.

Considering the stochastic nature of our energy-minimizing procedure, and in order to get statistical information about the number of MCS's required to observe the reversal of the system, we calculated 9×10^3 independent relaxation processes in order to evaluate (1) the frequency distribution of reversal events (i.e., the negative saturation) and (2) the average time (number of MCS's) evolution of the total magnetization of the system. The results for the distribution of reversal events are plotted in Fig. 3. The value obtained for the lifetime of the unreversed state was stable

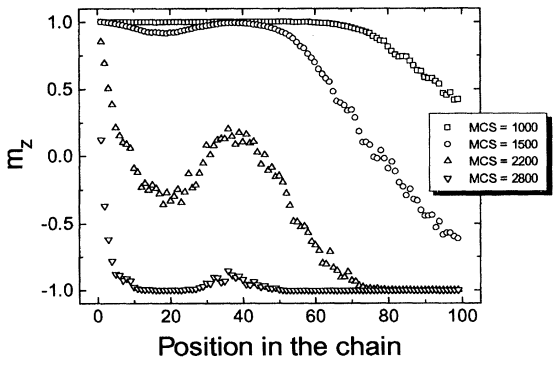

FIG. 2. System A. System configurations observed along the relaxation process. We have plotted the component along the field direction of the reduced magnetic moments representing the different planes in the system as a function of their position in the chain of planes.

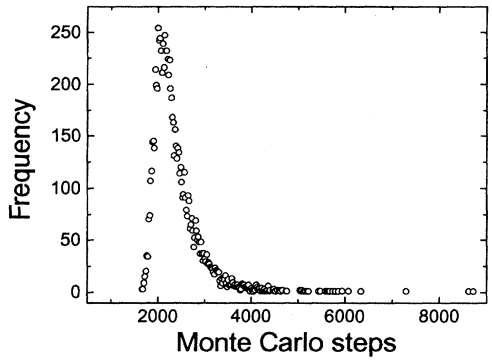

FIG. 3. System *A*. Distribution of reversal events plotted as a function of the number of MCS's.

after 10^3 independent runs of the relaxation process. The probability of magnetization reversal after a given number of MCS's (obtained by integration of the results in Fig. 3) is shown in Fig. 4. This probability is zero for a number of MCS's less than 1500. This marks a clear difference with the classical Arrhenius description of relaxation for which the probability is nonzero for arbitrarily small times.[14] In fact, our results clearly show the occurrence of a "waiting time," already observable in Fig. 1, during which the thermally induced magnetization fluctuations are either not stable or not able to produce the relaxation (i.e., not able to initiate the reversed magnetization nucleus). In order to highlight the difference between the calculated probability and that predicted by Arrhenius kinetics we also show in Fig. 4 the curve $[1-\exp(-N_{\mathrm{MCS}}/\langle N_{\mathrm{MCS}}\rangle)]$ where $\langle N_{\mathrm{MCS}}\rangle$ is the average value corresponding to the distribution in Fig. 3.

The average time evolution (number of MCS's) of the total magnetization component along the applied field is shown in Fig. 5. The data correspond to an average carried out over 500 independent runs of the relaxation process. One sees that magnetization evolution is far from the exponential decay corresponding to identical, noninteracting two-level systems.

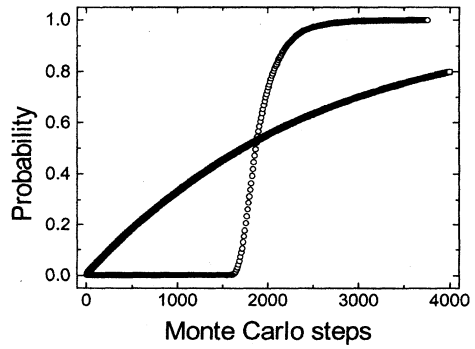

FIG. 4. System *A*. Probability of magnetization reversal as a function of the number of MCS's. For the sake of comparison, the Arrhenius prediction for the average number of MCS's required to accomplish the reversal (calculated from the distribution in Fig. 3) is also presented as the curve with finite slope at the origin.

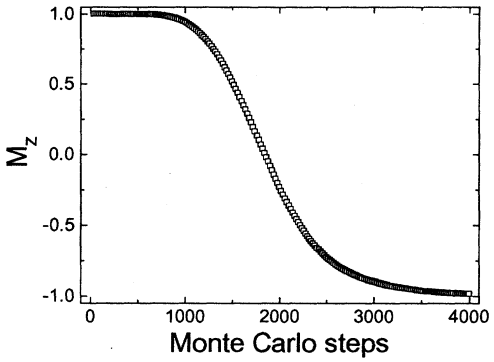

FIG. 5. System *A*. Average evolution of the reduced magnetization as a function of the number of MCS's.

B. Relaxation of a system with short-range coupling

Consider now two coupled grains whose easy axes are mutually perpendicular and both of them parallel to the grain boundary plane. In one of the grains the easy axis is directed parallel to the *OZ* axis of our reference system and the applied demagnetizing field H_{app} points along the negative *OZ* direction (the geometry of the system is illustrated in Fig. 6). This particular configuration is characterized by the fact that the orientation of the magnetic moments parallel to the plane of the interface is favored. Then, a small derivative with respect to the position of the component of the magnetic moments perpendicular to that interface is expected which has as a consequence the fact that the magnetostatic energy stored in the system should be much smaller than the other energies involved in the problem. As a consequence, intergranular coupling is mainly related to exchange.

In Fig. 6 we present the evolution of the reduced magnetization of the system with the number of Monte Carlo steps for $a=5.0$, $m=0.3$, $g=0.8$, $d=2.5\times10^{-10}$ m, and $H_{\mathrm{app}}=0.47$. This field value was slightly lower than the coercive force of a hysteresis loop calculated by decreasing the field from the positive saturation in steps of $\Delta H_{\mathrm{app}}=10^{-3}$ and allowing a relaxation at each field value of 5×10^3 MCS's (as discussed in Ref. 19 the intergranular exchange

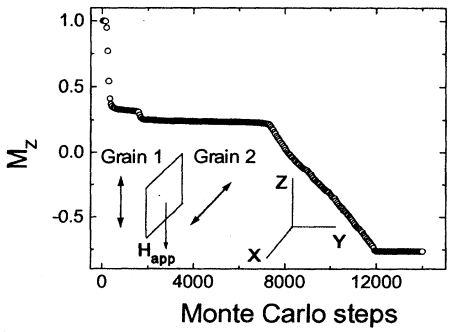

FIG. 6. System *B*. Typical example of the evolution of the reduced magnetization with the number of MCS's. Magnetization is measured along the *OZ* direction and it is considered positive when it points antiparallel to the applied magnetic field.

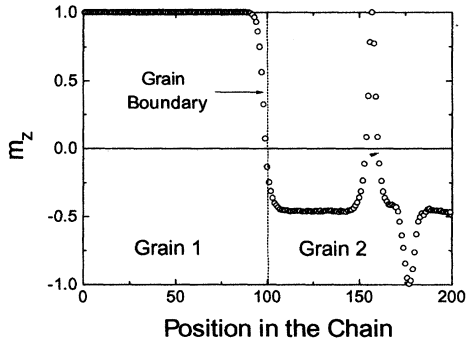

FIG. 7. System *B*. Configuration observed before the global magnetization reversal occurs. We have plotted the component along the field direction of the reduced magnetic moments representing the different planes in the system as a function of their position in the chain of planes (the grain boundary is located at position 100 in interplanar distance units).

coupling significantly reduces the field value at which irreversibilities occur, which in the present case and in the absence of intergranular exchange should be $H_{app}=1$). As is apparent from the figure, after an initial thermalization from the positive saturation, the system stays in remanence-type states for, approximately 7000 MCS's and then decays (irreversibly) towards a globally reversed state. There are a few points to comment on regarding the results in this figure. First, the remanence-type states corresponded, essentially, to a distribution of moments in which most of those in the left-hand grain (with easy axis directed parallel to the field direction) pointed antiparallel to the field, whereas those in the right-hand grain were directed along an intermediate direction between that of the local easy axis and the field direction. Also, a transition structure for the directions of the magnetic moments at the grain boundary region was formed. Obviously that structure is required to minimize the total internal energy since it enables the exchange energy to be significantly reduced. A second interesting point is that there exists a distribution of almost energetically equivalent remanence-type states: a transition between two of these states takes place at ca. 1600 MCS's in our relaxation example shown in Fig. 6. The equivalent states differ in the presence (see Fig. 7) or absence of structures clearly analogous to 360° domain walls which allow the magnetostatic contribution to the total internal energy to be minimized. The third point is that, as in the case of system *A*, relaxation takes place through propagation of a domain-wall-like structure (the interfacial transition structure, which unpins from the grain boundary, transforms into a 180° domain-wall-like structure and sweeps that grain; see Fig. 8) into the grain in which the moments point antiparallel to the demagnetizing field.

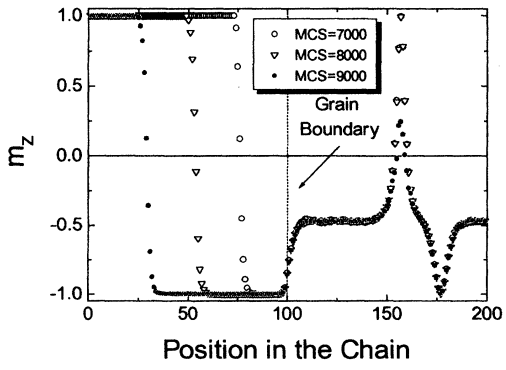

FIG. 8. System *B*. Propagation of a 180° domain-wall-like structure leading to the global reversal of the system (the grain boundary is located at position 100 in interplanar distance units).

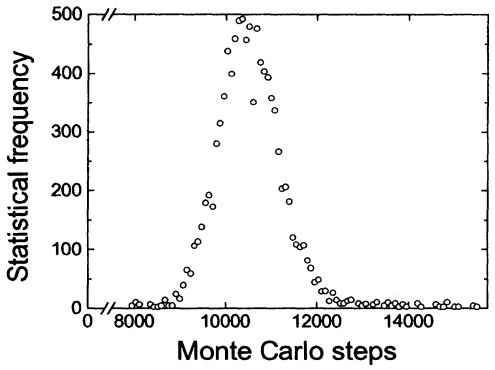

FIG. 9. System *B*. Distribution of reversal events plotted as a function of the number of MCS's.

All these three points clearly indicate that relaxation proceeds through the formation of finite structures in which a considerable number of degrees of freedom are involved.

Our results for the distribution of reversal events in system *B* (10^4 independent relaxation runs) are shown in Fig. 9 where the statistical frequency is plotted as a function of the number of MCS's. As in the case of system *A*, the reversal event is associated with the achievement of the minimum-energy state (which in the system under consideration and for the applied field value did not correspond to negative saturation).

In Fig. 10 we have plotted the probability of magnetization reversal after a given number of MCS's (obtained by integrating the results in Fig. 9). The average time evolution

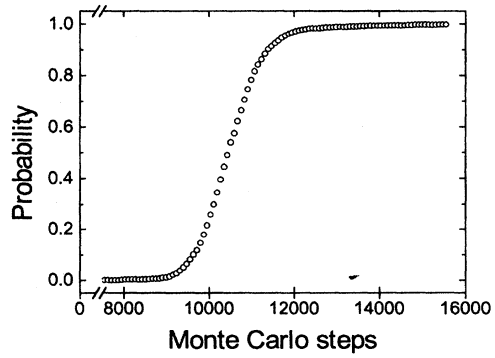

FIG. 10. System *B*. Probability of magnetization reversal as a function of the number of MCS's.

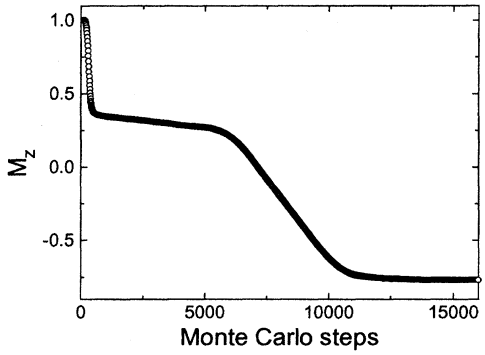

FIG. 11. System *B*. Averaged evolution of the reduced magnetization as a function of the number of MCS's.

(number of MCS's) of the magnetization component along the applied field direction is shown in Fig. 11. The data correspond to an average carried out over 200 independent runs of the relaxation process. The initial thermalization of the system has been included in the figure in order to give an idea about the number of steps required by our Monte Carlo algorithm to modify the state of the system in a case in which barriers are not involved.

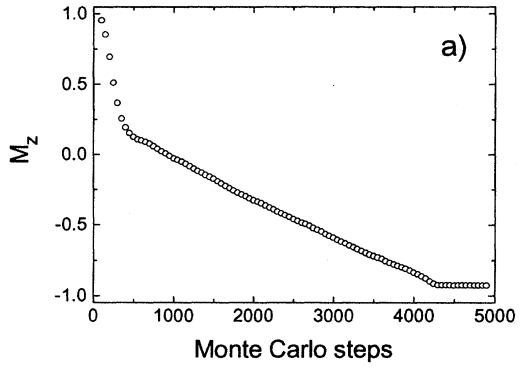

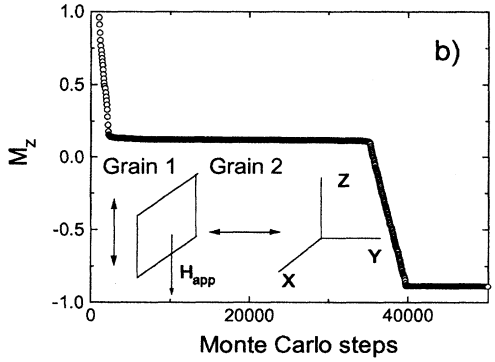

FIG. 12. System *C*. Examples of the (a) fast- and (b) slow-relaxation processes.

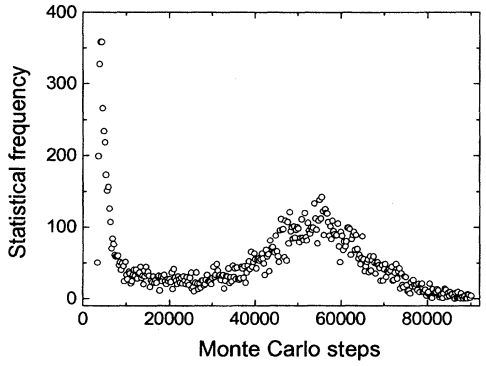

FIG. 13. System *C*. Distribution of reversal events plotted as a function of the number of MCS's.

C. Relaxation of a system with many-body interactions

Our third system (*C*) is again a two-grain system with mutually perpendicular easy axes. As in the case of system (*B*) one of the easy axes is parallel to the *OZ* axis, whereas the second one points perpendicularly to the plane of the interface [see an illustration of the geometry of the system in Fig. 12(b)]. The concrete parameters used in the relaxation study were $a=5$, $m=0.15$, $g=0.8$, $d=2.5\times10^{-10}$ m, and $H_{app}=0.51$. In contrast to system *B*, the particular easy-axes configuration here is such that one expects a gradual change across the interface of the component of the magnetic moment direction perpendicular to that interface. Therefore the grains in system *C* are both exchange and magnetostatically coupled. In Figs. 12(a) and 12(b) we present two typical examples of the evolution of the magnetization of system *C* with the number of MCS's. Apart from the very different number of MCS's corresponding to the reversal event, it is especially remarkable that in the case of Fig. 12(a) the system undergoes relaxation through a process clearly distin-

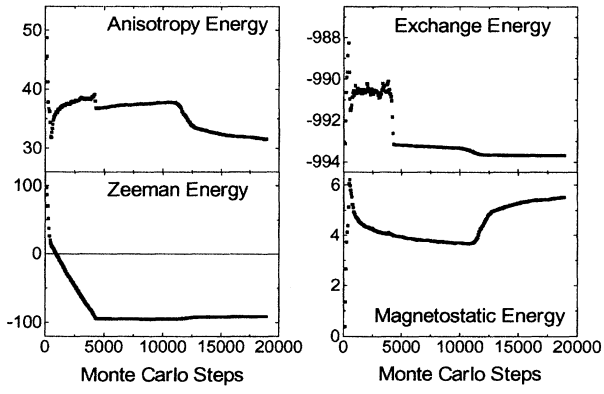

FIG. 14. System *C*. Fast-relaxation process. Evolution with the number of MCS's of the different energy terms describing the system (absolute energy units are arbitrary but the same for all the different combinations).

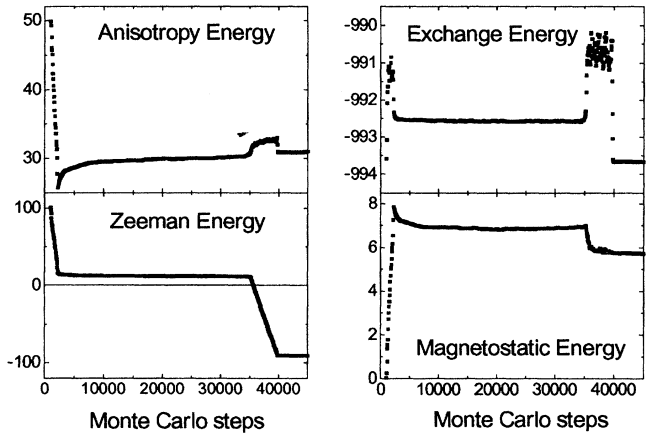

FIG. 15. System *C*. Slow-relaxation process. Evolution with the number of MCS's of the different energy terms describing the system (energy units as in Fig. 14).

guishable from that corresponding to Fig. 12(b): in this second case the system is trapped for a long MCS interval in a remanent-type state whereas in the first one thermalization is immediately followed by the accomplishment of the reversal.

The distribution of relaxation events (1.7×10^4 independent runs; Fig. 13) confirmed in statistical terms the occurrence of two nonequivalent relaxation paths since, as it is possible to conclude from the figure, the fast relaxation processes are clearly distinguishable from the tails of the slow-processes distribution (see Fig. 13).

In order to identify the nature of these two inequivalent trajectories we have followed (in two particularly fast and slow relaxation runs) the evolution of the different energy terms involved in the total free energy. The results are plotted in Figs. 14 (fast-relaxation case) and 15 (slow-relaxation case). The most remarkable difference between the two sets of data is related to the magnetostatic energy. In the fast-relaxation case, the system, after thermalization, suffers a large (in percentage) reduction of that term which, from the examination of the magnetic moment configuration, is identified as corresponding to the formation of undulations of the magnetic moments in the grain in which the local easy axis points along the *OY* direction of our reference system (Fig. 16). Those undulations, although effective in reducing the magnetostatic energy (through the increase of the order of the total multipolar moment of the system), provide a sufficient degree of magnetic moment direction inhomogeneity so as to render the system highly unstable against thermal fluctuations. On the other hand, in the case of slow relaxation, the system gets trapped in a state in which magnetic poles are more localized at the interfacial region. According to Fig. 16 the magnetostatic energy corresponding to that remanence-type state can only be lowered when propagation of the transition structure at the interface occurs. The final energy values reached after both were the same (to within the resolution of the calculation).

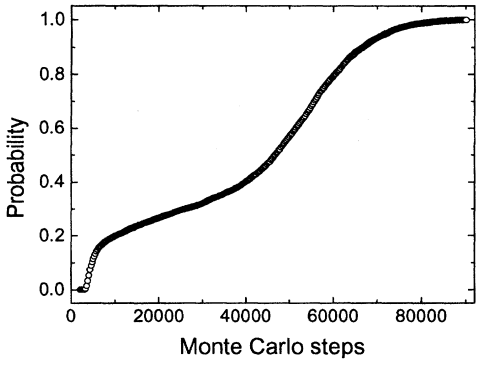

FIG. 17. System *B*. Probability of magnetization reversal as a function of the number of MCS's.

The probability of magnetization reversal as a function of the number of MCS's evaluated from the results for the distribution of reversal events is shown in Fig. 17. In contrast to system *B*, the fast-relaxation mode makes a nonzero reversal probability for short times (small number of MCS's) possible. Nevertheless, we should point out that, strictly speaking, a "waiting time," similar to that observed in the previously discussed systems, is also detected here. The reversal probability linked to the activation of the slow process seems to evolve with the number of MCS's in a similar way (except

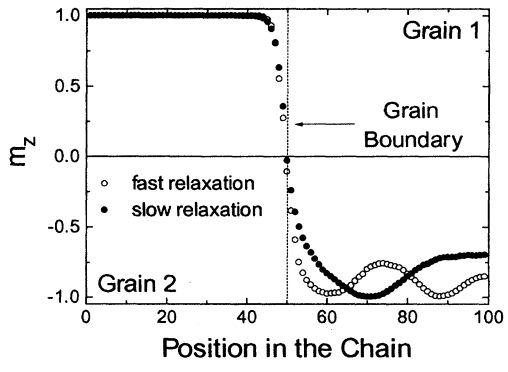

FIG. 16. System *C*. Reduced magnetic moment distributions observed, before the global reversal, in the cases of the fast and slow relaxation (the grain boundary is located at position 50 in interplanar distance units).

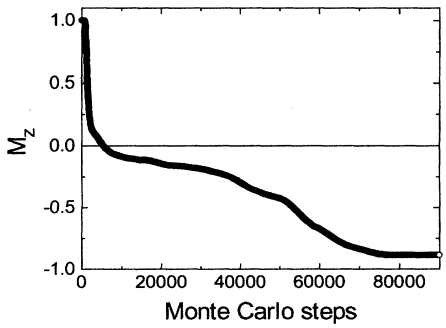

FIG. 18. System *B*. Averaged evolution of the reduced magnetization as a function of the number of MCS's.

for the scales involved) to that described in the case of system *B*. Finally, a plot of the evolution with the number of MCS's of the magnetization of system *C* (average evolution over 500 independent runs, initial thermalization process plotted) is presented in Fig. 18. The complexity of this evolution clearly highlights the limitations of Arrhenius kinetics when applied to describe magnetic relaxation.

III. CONCLUSIONS

From our results the following conclusions can be drawn. (1) Like hysteresis, magnetic relaxation of simple systems occurs through the formation and propagation of structures (of the domain-wall type) involving a fraction of the total number of magnetic moments of the system. (2) The relaxation of one of these model systems possessing many degrees of freedom cannot be qualitatively described in terms of a two-level system. Although the transition from a metastable state to a stable state in a complex energy surface could, in some cases, be described as a simple transition between two levels (ignoring, for instance, the possible corrugation of that energy surface in the region close to the local minimum) the crucial difference is the possibility of inequivalent (either not simply connected or, as we observed in the case of system *B*, involving clearly distinct time scales) trajectories linking those minima. (3) The time evolution of the magnetization depends markedly on the involved interactions but in the three cases we studied here it cannot be described in terms of Arrhenius kinetics. In particular, the occurrence of a very slow (if compared to the Arrhenius predictions) relaxation rate prior to the propagation of the magnetic moment structures responsible for the global magnetization reversal (a "waiting time" which seems to be in agreement with the experimental results presented in Ref. 20 for the relaxation of an individual single-domain particle) and the clear evidence of the occurrence of distinguishable relaxation trajectories (which in system *C* were identified as linked to the dipolar energy) support the idea[21] that a two-level-system description of the relaxation in systems bearing many degrees of freedom is far from being realistic.

[1] D. W. Taylor, V. Villas-Boas, Q-Lu, M. F. Rossignol, F. P. Missell, D. Givord, and S. Hirosawa, J. Magn. Magn. Mater. **130**, 225 (1994).

[2] H. Kronmüller, in *Science and Technology of Nanostructured Magnetic Materials*, edited by G. C. Hadjipanayis and G. A. Prinz (Plenum, New York, 1991), p. 657.

[3] R. Street, P. G. McCormick, and L. Folks, J. Magn. Magn. Mater. **104–107**, 368 (1992).

[4] K. O'Grady, R. W. Chantrell, J. Popplewell, and S. W. Charles, IEEE Trans. Magn. **MAG-17**, 2945 (1981).

[5] S. B. Oseroff, D. Clark, S. Schultz, and S. Shtrikman, IEEE Trans. Magn. **MAG-21**, 757 (1984).

[6] D. Givord, P. Tenaud, T. Viadieu, and G. C. Hadjipanayis, J. Appl. Phys. **61**, 3454 (1987).

[7] R. Street, R. K. Day, and J. B. Dunlop, J. Magn. Magn. Mater. **69**, 106 (1987).

[8] J. C. G. Martínez, F. P. Missell, and F. J. G. Landgraf, J. Magn. Magn. Mater. **73**, 267 (1988).

[9] P. K. Lottis, E. Dan Dahlberg, J. A. Christner, J. I. Lee, R. L. Peterson, and R. M. White, J. Appl. Phys. **63**, 2920 (1988).

[10] M. P. Sharrock, IEEE Trans. Magn. **25**, 4374 (1989).

[11] M. P. Morales, C. de Julián, C. J. Serna, and J. M. González, IEEE Trans. Magn. **30**, 792 (1994).

[12] Y. Kanai and S. H. Charap, IEEE Trans. Magn. **27**, 4972 (1991).

[13] J. M. González-Miranda and J. Tejada, Phys. Rev. B **49**, 3867 (1994).

[14] L. Néel, Adv. Phys. **4**, 191 (1955).

[15] R. W. Chantrell, J. Magn. Magn. Mater. **95**, 365 (1991).

[16] A non-Arrhenius relaxation mechanism has been recently proposed by R. V. Chamberlin and M. R. Scheifein [Ultramicroscopy **47**, 408 (1992)] and R. V. Chamberlin [Phys. Rev. B **48**, 15 638 (1995)].

[17] E. C. Stoner and E. P. Wohlfarth, Philos. Trans. R. Soc. London Ser. A **240**, 599 (1948).

[18] J. M. González, R. Ramírez, R. Rueda, L. Domínguez, and J. González, IEEE Trans. Magn. **30**, 4359 (1994).

[19] A. Hernando, I. Navarro, and J. M. González, Europhys. Lett. **20**, 175 (1992).

[20] M. Lederman, D. R. Fredkin, R. O'Barr, S. Schultz, and M. Ozaki, J. Appl. Phys. **75**, 6217 (1994).

[21] M. Lederman, S. Schultz, and M. Ozaki, Phys. Rev. Lett. **73**, 1986 (1994).